Photoemission study of the valence band of Pb monolayers on Ge(111)

B. P. Tonner,* H. Li, and M. J. Robrecht
Department of Physics and Laboratory for Surface Studies, University of Wisconsin–Milwaukee, Milwaukee, Wisconsin 53201

Marshall Onellion and J. L. Erskine
Department of Physics, University of Texas, Austin, Texas 78712
(Received 12 December 1986)

Monolayers of Pb have been grown epitaxially on clean Ge(111) surfaces. The metal overlayer reorders the surface and results in a $(\sqrt{3}\times\sqrt{3})R30°$ unit cell. The valence-band dispersions of this metal-semiconductor interface system have been measured with use of angle-resolved photoemission spectroscopy with synchrotron radiation. The Pb/Ge(111) overlayer remains semiconducting, as reflected in the valence-band density of states at the Fermi level. Two lead-induced surface states are found, which are related to surface states seen in the clean, reconstructed Ge(111)-$c(2\times8)$. The binding energies of these states, relative to the valence-band maximum, are 0.45 and 1.2 eV. A small bandwidth of 0.3 eV is found for the deeper state. The similarity of the Pb-induced surface state bands to those of clean, reconstructed Ge(111)-$c(2\times8)$ suggests that there is a corresponding similarity in surface geometric structure. These experimental findings support an adatom model of the clean Ge reconstruction in the same way that Si(111)$(\sqrt{3}\times\sqrt{3})$-metal overlayer structures have supported the adatom model for Si(111)-(7×7). A structure for Pb/Ge(111) incorporating Pb adatoms on threefold-coordinated T_4 or H_3 sites is proposed.

I. INTRODUCTION

Clean surfaces of Ge(111) exhibit a variety of reconstructions that depend upon sample treatment.[1–3] A surface that is ion sputtered and annealed, for example, will produce a surface reconstruction that is commonly indexed according to its low-energy electron diffraction (LEED) pattern as three domains of $c(2\times8)$.[4–6] A recent proposal[7] has been made that interprets the reconstruction as being based upon a dimer-adatom-stacking fault (DAS) model that bears a strong similarly to one proposed for the Si(111)-7×7 reconstruction.[8,9] A key feature of the DAS models is the presence of adatom bonding sites that saturate three dangling bonds of the unreconstructed surface, and have a local tetrahedral bonding symmetry. The metallic elements Sn and Pb, which occur in the same group of the Periodic Table as Si and Ge, can be epitaxially grown on the Ge(111) surface.[10] In this paper we present experimental measurements of the electronic properties of monolayer Pb films on Ge(111) surfaces, and discuss the relationship of our results of the DAS model of the clean Ge(111) reconstruction.

Monolayers of Pb on Ge(111) result in a LEED pattern that has a $(\sqrt{3}\times\sqrt{3})R30°$ unit cell.[11–13] A structural model for this metal-semiconductor interface is shown in Fig. 1. Lead atoms are shown occupying threefold occupied sites with locally tetrahedral symmetry (T_4) on an unreconstructed Ge(111) surface. The geometry illustrated is one of several possible that are consistent with a $\sqrt{3}\times\sqrt{3}$ LEED pattern. The $\sqrt{3}\times\sqrt{3}$ superlattice unit cell of Pb/Ge(111) is also seen in the overlayer systems of Al/Si(111),[14] Ga/Si(111),[15] In/Si(111),[16] Ag/Ge(111),[17] and Sn/Ge(111).[10] Our results of measurements of the surface band structure of the lead system indicate that there is an overall similarity in the electronic properties of these overlayers, in addition to the correspondence in structure.

From an experimental standpoint, the Pb/Ge system has several attractive features as a model for the study of interface properties. It is possible to establish overlayer deposition conditions that reproducibly give monolayer coverage with high accuracy, as corroborated by several spectroscopic techniques. The solid solubility of lead in germanium is negligible,[18] so that the interface is well defined over all temperatures for which lead does not desorb, without complications due to alloying or dissolution into the bulk. The melting point and Debye temperature of Pb surfaces is much lower than that of Ge, which makes the Pb/Ge(111) system useful in studies of the temperature dependence of surface properties. There is some evidence from electron diffraction that the Pb overlayer undergoes a melting phase transition at $T=192\,°C$,[12] although an alternative explanation of the transition is that it is a solid-solid structural change.[11,13] Along these lines, we point out that Pb on Ge(111) should be an excellent candidate for surface x-ray scattering experiments of two-dimensional phase transitions.[19] The overlayer has a high Z, leading to large scattering amplitudes, and the substrate is a high-quality semiconductor crystal exhibiting excellent long-range order and surface flatness.

Previous work on the Pb/Ge(111) overlayer system has concentrated primarily on electron diffraction studies. Ichikawa has employed reflection high-energy electron diffraction (RHEED) to study both the Sn and Pb monolayer coverages on Ge(111).[10,12] In the Pb case, a solid-liquid phase transition was proposed, based on the azimuthal isotropy of fractional order RHEED beams above the phase transition.[12] Ichikawa argued that the absolute cov-

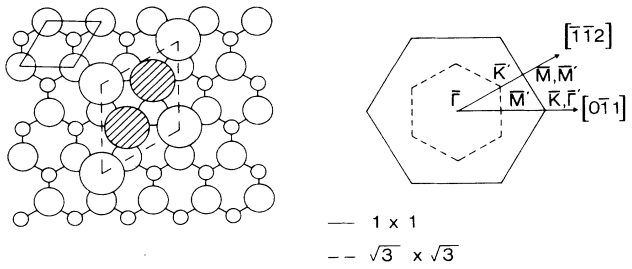

FIG. 1. Real-space model of Pb/Ge(111) and momentum-space unit cells. In the real-space diagram, the large open circles represent Pb atoms on a $\sqrt{3}\times\sqrt{3}$ lattice with a coverage of $\Theta=\frac{1}{3}$, the shaded circles are possible additional Pb atom sites for higher coverage. The medium-size and small open circles represent the first two layers of an ideal Ge(111) surface.

erage Θ for the saturated monolayer was $\frac{4}{3}$. Here Θ is defined as the ratio of the number of Pb adatoms to Ge surface layer atoms. Additional experiments involving Auger spectroscopy and observation of LEED patterns have been performed by LeLay *et al.*[11,13] This group disagrees with the identification of the nature of the phase transition, ascribing it instead to a solid-solid structure change. LeLay assigns a coverage of $\Theta=1$ to the monolayer.[11]

We have performed a series of photoelectron spectroscopy experiments of the saturated monolayer to determine the surface band structure for comparison to that of bulk lead and germanium. A tandem set of experiments were performed using LEED I-V spectra as a function of lead coverage to determine the overlayer structure. The experimental I-V curves for 10 fractional and integer order beams and coverages ranging from $\frac{1}{2}$ to 10 monolayer thickness will appear elsewhere.[20]

II. EXPERIMENTAL METHOD

The germanium substrate material was antimony-doped 5–10-Ω-cm-resistivity (111)-oriented wafers of 0.5 mm thickness. Sections of the original wafer were diced into approximately 10×5 mm^2 pieces and mechanically polished using diamond and alumina suspensions. The sample was mounted to a Ta foil backing strip using Ta clips. The substrate was heated by passing a current through the Ta mounting foil. Substrate temperatures could be monitored by a thermocouple attached to the foil backing, which was calibrated at higher temperatures by comparison to the reading from an optical pyrometer focused on the center of the crystal surface. Clean Ge(111) surfaces were obtained by several cycles of Ar-ion bombardment (1 keV) followed by annealing at $\approx$800 °C for several minutes. The surface cleanliness was determined by measuring the Auger electron spectrum, taking particular care to guarantee the absence of C, O, or Ta contaminants. The surface order of clean Ge was monitored by both LEED and angle-resolved photoelectron spectroscopy (ARPES). In the LEED pattern, $\frac{1}{2}$-order spots appeared early in the cleaning cycle. After several sputter and anneal cycles, diffuse intensity centered on the $\frac{1}{8}$-order spot locations appeared, when the LEED screen pattern was viewed by eye. Photographs of similar patterns taken in a separate experiment using the same samples showed definite sharp $\frac{1}{8}$-order spots, with much weaker intensity than the $\frac{1}{2}$-order beams. The clean surface of Ge(111)-$c(2\times8)$ was examined using ARPES, in order to reproduce the details of previous work on this surface.[21–28] In particular, the two low-binding-energy surface states apparent, for example, at normal emission with 17-eV photon energy were reproduced,[26] as was the angular distribution of photoemission along the $[0\bar{1}1]$ direction using 21.2-eV photon energy.[25]

ARPES measurements of the surface and bulk band structure of clean and Pb-covered Ge(111) were performed using an angle-resolving hemispherical electron energy analyzer[29] and two-axis goniometer. Unpolarized He I resonance lamp radiation of 21.2-eV energy was used in addition to synchrotron radiation at the University of Wisconsin Synchrotron Radiation Center (Stoughton, WI). Two monochromators were employed, a Seya-Namioka device for low-energy experiments ($12\leq\hbar\omega\leq30$ eV) and a toroidal grating monochromator for low and medium energies ($20\leq\hbar\omega\leq80$ eV).[30] A combined energy resolution with contributions from photon source and electron spectrometer of 0.3 eV was maintained.

The crystal was oriented with the $[0\bar{1}1]$ direction parallel to the plane of polarization of the synchrotron radiation. Photoelectron angular distributions were collected at various polar angles in the plane of polarization $[0\bar{1}1]$, and perpendicular to the plane of polarization along the $[\bar{1}\bar{1}2]$ bulk crystallographic direction. The angle of incidence of synchrotron radiation for the in-plane polar-angle distributions was typically 45°, that for the unpolarized resonance lamp experiments was fixed at 22.5°.

An important aspect of all epitaxial growth experiments is an accurate and reproducible determination of the overlayer coverage. In these experiments, lead of 99.999% purity was evaporated from a quartz cup, indirectly heated by a tungsten filament. The temperature of the tungsten filament was measured by a thermocouple. Lead evaporation rates could be monitored by a quartz microbalance placed midway between the sample and the lead oven. Since the microbalance is not located at the sample position, an alternative determination of Pb exposure at the sample is necessary. This was obtained by measuring the Auger electron yield from Ge and Pb atoms as a function of relative exposure to lead as determined from the frequency change of the quartz microbalance. The results of a typical run are shown in Fig. 2. It is quite common in systems that exhibit layer-by-layer growth to find Auger yield curves that exhibit slope changes at the point of completion of a layer.[31] As can be easily seen in Fig. 2, in our case this slope change is quite large, due to the short mean free path of low-energy electrons in lead. This large effect enables us to accurately determine first-layer completion to ±10%. An additional check on coverage is obtained by monitoring the fractional order LEED beams as a function of Pb coverage. As the monolayer nears completion the intensity of the $(\frac{2}{3},\frac{2}{3})$-order beams increases and the $(\frac{1}{3},\frac{1}{3})$-order beams become very weak.[11]

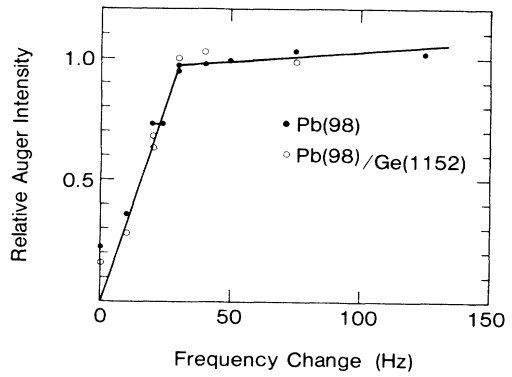

FIG. 2. Auger electron yield from Pb/Ge as a function of relative coverage as determined by the frequency change of a quartz-crystal microbalance. The measured intensity is not zero for zero exposure because of an unresolved overlap of Ge and Pb Auger lines.

Also, the intensity of $(\frac{2}{3},\frac{2}{3})$-order LEED diffraction spots for monolayer coverage was measured as a function of substrate temperature. It has been previously determined that the temperature dependence of these spots is a function of overlayer coverage.[11–13] The diffraction intensity in our experiments shows a discontinuity in slope (after removing the Debye-Waller contribution) at 190±10 °C, in agreement with previous results for saturated monolayers.

This procedure does not, however, determine the absolute coverage, defined as the ratio of Pb atoms to surface Ge atoms. A commensurate monolayer of fcc (111) surface Pb can be accommodated on the Ge(111) surface with a change in lattice constant of 1%. This would result in an absolute coverage of $\Theta=\frac{4}{3}$. Such a structure would require a thick film of lead to grow with Pb[1$\bar{1}$0]||Ge[$\bar{1}\bar{1}$2], which we do not observe in the LEED pattern of thick films. Instead, commencing with the second layer we find LEED superlattice spots corresponding to fcc Pb(111) with an orientation of Pb[1$\bar{1}$0]||Ge[1$\bar{1}$0]. These superlattice spots are accompanied by weaker satellite spots due to domains rotated by $\approx\pm4°$.[32] The rotated domains may result from a contraction of the multilayer film towards the smaller unit-cell size of pure lead. There is no evidence in the multilayer films for LEED spots corresponding to an epitaxial structure growing on a $\Theta=\frac{4}{3}$ monolayer, so we exclude this coverage from consideration.

In a separate LEED experiment, a quartz microbalance was located at the sample position to establish the lead flux corresponding to monolayer completion. These experiments found a completed monolayer occurs for $\Theta=1$, although we do not expect the microbalance to be more accurate than of order 50%. A coverage of $\frac{2}{3}$ is achieved in the structure shown in Fig. 1, with one of the shaded lead atom sites occupied in addition to the four corner sites. This structure has been called a honeycomb lattice because of the appearance of the empty holes. Placing Pb atoms at both of the shaded sites in Fig. 1 results in a coverage of $\Theta=1$. Therefore, these atoms must be made inequivalent to the corner atoms by horizontal or vertical displacements from the true threefold sites to preserve the $\sqrt{3}\times\sqrt{3}$ LEED pattern. The structural model of Fig. 1 is compatible with the observation of [1$\bar{1}$0]||[1$\bar{1}$0] epitaxy. Both the honeycomb structure with $\Theta=\frac{2}{3}$ and the filled $\Theta=1$ structure fall within the limits of accuracy of our measurement of the absolute coverage from microbalance measurements.

At this time, the value of the absolute coverage obtained at completion of the first monolayer of Pb is not universally agreed upon. However, it must be emphasized that the Auger yield data demonstrate that reproducible saturated monolayers can be reliably grown and a comparison of results of various spectroscopies studying the saturated monolayer is possible. In this paper we argue that the measured surface band structure of Pb/Ge(111) requires threefold coordinate Pb atoms, which provides a starting point for future structural analyses, and excludes structures with atoms occupying bridge sites.

III. RESULTS

Figure 3 shows a representative set of spectra taken with unpolarized He I radiation. Photoelectron energy distribution curves (EDC's) are plotted as a function of polar angle. The plane of incidence of the light, and the emission plane of the electrons, are parallel to the bulk Ge[1$\bar{1}$0] direction. Binding energies are referenced to the valence-band maximum (VBM) throughout this paper. These spectra show two features with nearly constant binding energy at 0.45±0.05 and 1.2±0.1 eV below the VBM. We argue below that these two states are surface

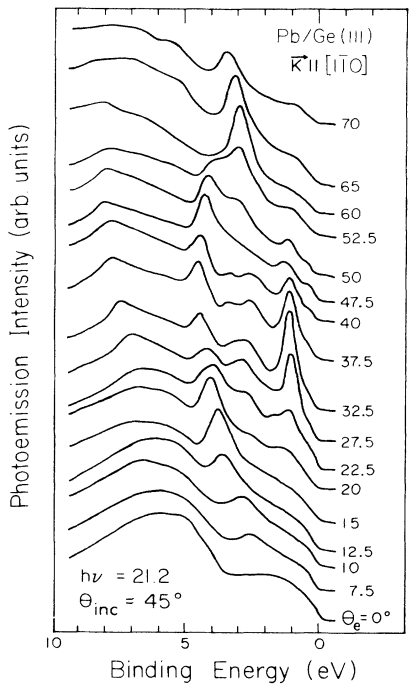

FIG. 3. Energy distribution curves of monolayer Pb/Ge(111) using unpolarized He I radiation, as a function of electron polar angle θ_e.

states of the Pb/Ge complex. In addition, there are several higher-binding-energy states that show significant dispersion, in the energy range from 2 to 8 eV below VBM, which are related to the bulk Ge band structure.

The spectra of Fig. 3, taken with unpolarized light in a plane which is not a mirror plane of the bulk, should exhibit the most general emission from the sample since no significant selection rule is in force. It is apparent from these characteristic EDC's that the lead-covered Ge surface does not become metallic, since the density of states (DOS) at the Fermi level (established in terms of the electron kinetic energy by the work function of the electron spectrometer) remains unchanged from that of clean, semiconducting Ge. A direct comparison to pure Pb(111) can be made using the data of Horn *et al.*[33] They show that a state in Pb(111) crosses the Fermi level for normal emission ($\Theta_e=0$) at a photon energy of 22 eV. This state is clearly absent in our spectra for Pb/Ge(111) at 21.2 eV. Indeed, at no photon energy studied in the range 13–70 eV has any significant intensity at E_F been seen.

Detailed polar-angle-dependent EDC's were accumulated with synchrotron radiation at 13-, 17-, 21-, and 25-eV photon energy, in the plane containing the bulk [1$\bar{1}$0] direction. For orientation in momentum space, we refer to Figs. 1 and 4. Because of the complexity of the bulk Ge crystal and (111) surface, along with the changes induced by the Pb overlayer, there is a need to index several surface real-space and **k**-space unit cells. The structures shown in Fig. 1 are referenced to the lattice spacing of an ideal unreconstructed Ge(111) surface. Figure 4 shows a section of the *bulk* Brillouin zone in the (1$\bar{1}$0) plane. The notation for the surface Brillouin zone (SBZ) symmetry points is the same as that of Fig. 1. Also shown are the bulk high symmetry points that lie in the (1$\bar{1}$0) plane. Three bulk zones are encountered as $\mathbf{k}_\parallel$ varies from zero at normal emission to the nearest Γ point of the extended bulk Brillouin zone. The magnitude of perpendicular momentum (vertical axis in Fig. 4) is calculated from a free-electron model with a fixed inner potential (see Sec. IV below).

In Figs. 5 and 6 we illustrate some of the important EDC's from Pb/Ge(111) and clean Ge(111)-$c(2\times8)$ under various excitation conditions. The spectra in Fig. 5 were selected to represent emission for the same range of parallel momentum $\mathbf{k}_\parallel$ for three photon energies. A strong dependence on photon energy of the intensity and binding energy of several peaks in the (2–6)-eV binding energy (BE) range is indicative of direct transitions,[21] while the feature present at all three photon energies at 1.2-eV BE is identified as a Pb-induced surface state. The data of Fig. 6 show the strong correlation between features seen in the Pb/Ge complex and those seen under identical excitation conditions for reconstructed Ge(111)-$c(2\times8)$.

The dispersion of the bands seen in spectra from such polar-angle plots is summarized in Figs. 7 and 8. Data presented in Fig. 7 were collected at a single photon energy (21 eV), while Fig. 8 incorporates data from several photon energies (13, 21, and 25 eV) as discussed below. The value of parallel momentum used in generating Figs. 7 and 8 is calculated by assuming $\mathbf{k}_\parallel$ conservation and applying the formula $|\mathbf{k}_\parallel|=0.512(\sin\theta_e)(\hbar\omega-E_{\rm BE}-\phi)^{1/2}$. The value of the work function ϕ used in the band-structure analysis was chosen to be 4.3 eV as a compromise between the work function of Pb (3.8 eV) (Ref. 33) and Ge (4.8 eV) (Ref. 23); the calculated dispersions are relatively insensitive to variations in ϕ of 0.5 eV or so at the photon energies used in this work.

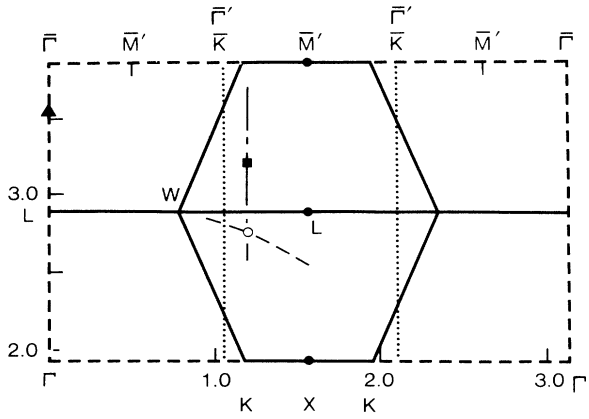

FIG. 4. Symmetry points of the bulk Ge(111) reciprocal space appropriate for the [1$\bar{1}$0] direction. The solid lines correspond to surfaces and edges of the bulk Brillouin zone; the dashed lines lie in the interior of reciprocal-space cells. The vertical lines marked $\bar{K}$ are the surface zone boundaries of bulk Ge. Primed symmetry points refer to a $(\sqrt{3}\times\sqrt{3})$ superlattice. The symbols are explained in the text.

The polarization dependence of emission from the valence band of Pb/Ge(111) was investigated, as shown in the data of Fig. 9. The sensitivity of the surface-state features to the component of light perpendicular to the surface was tested in two ways. In the top pair of spectra (*a* and *b*) the angle of incidence of the light is varied so as to change the relative magnitude of the in-plane surface

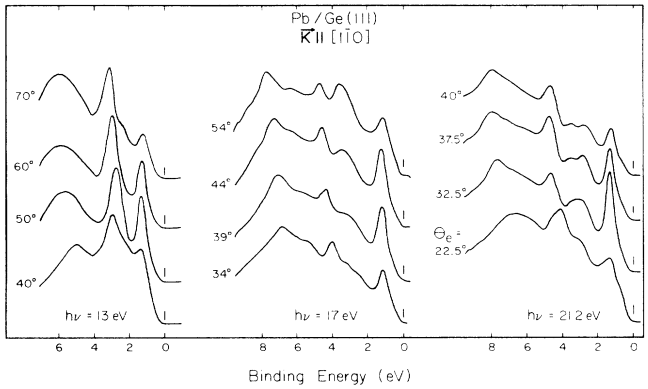

FIG. 5. A constant region of $k_\parallel$ is maintained in these three sets of curves by altering the range of electron polar angle θ_e sampled as the photon energy is changed. In each set of curves, a feature at $\approx$1.2-eV binding energy shows a strong dependence on polar angle, which corresponds in momentum space to an absolute band gap of bulk Ge.

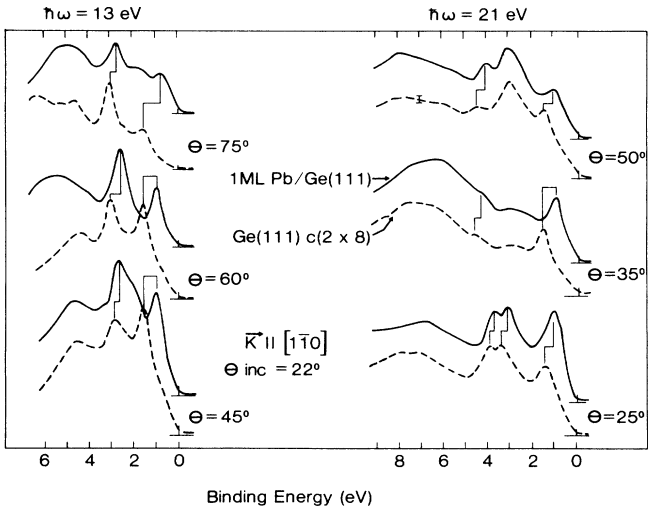

FIG. 6. Photoemission from clean Ge(111)-$c(2\times8)$ (dashed curves) compared to monolayer Pb/Ge(111) (solid curves) for a selection of polar angles and photon energies. Polarized synchrotron radiation is the light source.

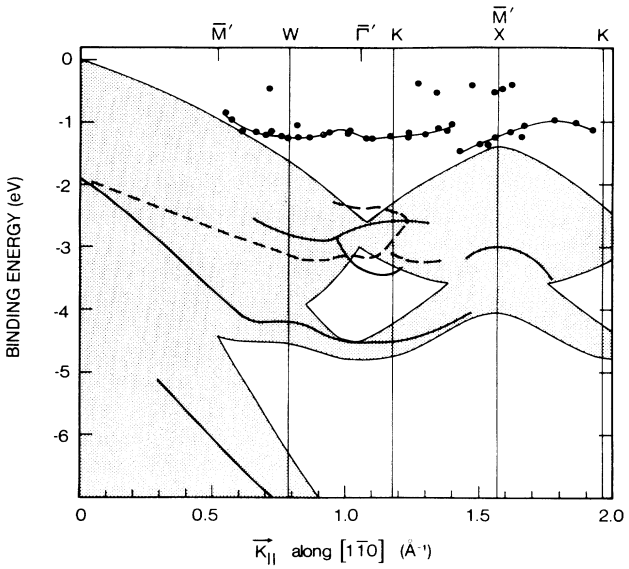

FIG. 8. Summary of dispersive peaks in Pb/Ge(111) from polar-angle scans at 13-, 17-, 21-, and 25-eV photon energy. The shaded area is the projection of the bulk Ge bands in the [1$\bar{1}$0] direction.

and normal components of the incident **A** vector, all other variables remaining the same. In both of the second pair of spectra (*c* and *d*) the **A** vector lies in the surface plane, but is either parallel or perpendicular to the emission direction of the electron. For both pairs of spectra, the intensity is scaled so that the peak at 7.5-eV BE is the same. These spectra indicate that the feature at 1.2-eV BE is enhanced by the A_z and in-plane components of the incident photon field. This behavior is indicative of an initial state with predominantly p_z character. A pure p_z state would have no intensity in the even-state forbidden geometry of Fig. 9 (spectra *d*), so that some additional contribution from p_x- and p_y-type orbitals is indicated by the presence of weak emission at 1.2 eV in this spectrum.

IV. DISCUSSION

Referring to Fig. 3, there are two low-binding-energy features at 0.45 and 1.2 eV. The 0.45-eV feature is visible only as a shoulder in most spectra, although a separate

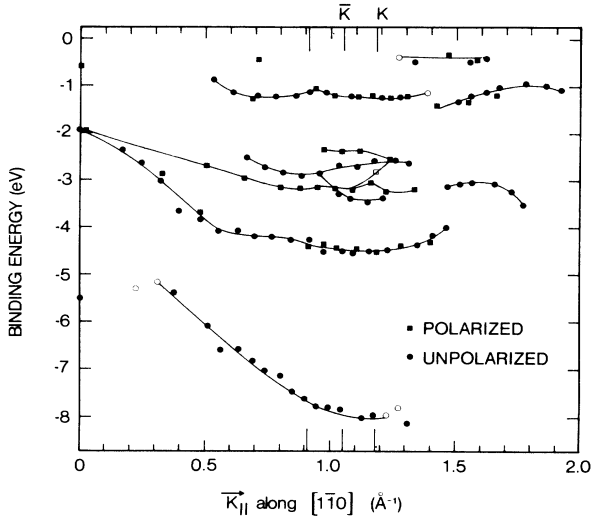

FIG. 7. Measured dispersions of features seen in Pb/Ge(111) at a single photon energy (21 eV). The squares mark features seen with polarized synchrotron radiation, circles were taken from He I data. Open figures represent weak structures or shoulders.

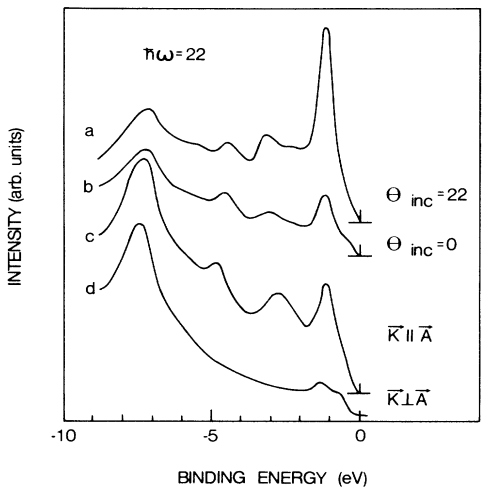

FIG. 9. Polarization dependence of the Pb/Ge(111) surface state. In the upper pair of spectra, the angle of incidence of the light is varied for constant electron polar angle of emission. The lower pair compares the same polar angle with light parallel or perpendicular to the emission direction. The polar angle of emission is 30° in all spectra.

peak is occasionally evident (see the $\theta_e = 47.5°$ EDC in Fig. 3, for example). It is clear in Fig. 3 that there is a strong angular dependence to the intensity of emission from the 1.2-eV state. As is well known, the intensity variations in angle-resolved photoemission may arise from several causes. A simple model for photoemission divides such effects into three contributions to the photoemission matrix element, i.e., initial state, operator, and final-state effects.[34]

In order to investigate the angular dependence of intensity further, polar-angle distributions were measured at several photon energies. A sampling of this data is shown in Fig. 5 (data accumulated at 25-eV photon energy was similar). The spectra of Fig. 5 were selected from the complete polar distribution ($0° \leq \theta_e \leq 80°$) so as to represent a *fixed* range of $\mathbf{k}_\parallel$ for all three photon energies. What is demonstrated is that the intensity variation is related to the region of $\mathbf{k}_\parallel$ momentum space sampled, but independent of the magnitude of $k_\perp$ (which varies with photon energy). A polar plot taken with a different angle of incidence of light confirmed that the intensity variation with angle of the 1.2-eV state is simply related to $\mathbf{k}_\parallel$, and not dependent on the direction of light polarization.

The range of momentum sampled by the spectra in Fig. 5 is approximately $0.8 \leq |\mathbf{k}_\parallel| \leq 1.3$ Å^{-1}. The peak at 1.2-eV BE is strong in both the unpolarized emission spectra and those taken with synchrotron radiation, for which the polarization vector lies in the plane of electron emission. The dispersion along $[1\bar{1}0]$ is shown in Fig. 7 for 21-eV photon energy. The peak at 1.2 eV shows a small amount of dispersion of approximately 0.3 eV. Although the small magnitude of this dispersion makes an identification of the symmetry point for this band difficult, there is an indication that the band is symmetric around the $\bar{\Gamma}'$ point of the $\sqrt{3}\times\sqrt{3}$ overlayer unit cell. This value of $\mathbf{k}_\parallel$ is indicated in Figs. 7 and 8, along with the points $\bar{K}$ and K, which are the ideal Ge(111) surface Brillouin zone (SBZ) boundary and projection of the bulk K point, respectively. The peak at 0.45 eV was only identifiable for a small number of polar angles, so that it is not possible to determine any dispersion for this feature.

Both the 0.45- and 1.2-eV peaks lie in a region of $\mathbf{k}$ space for which there are no bulk Ge bands. This is illustrated in Fig. 8 in which the projected bulk bands occupy the shaded region of the graph. We argue that the 1.2- and 0.45-eV states are surface states of the Pb/Ge complex as follows. That these two features lie in a bulk band gap is evident from Fig. 8. The dispersion of the 1.2-eV state is the same for all photon energies measured, indicating no dependence on the perpendicular component of the momentum. In experiments reported earlier, the temperature dependence of the intensity of photoemission from the surface states was measured.[35] There it was shown that the 1.2-eV state has a Debye-Waller intensity dependence with a characteristic temperature of 41 K, much lower than that of bulk Ge (but similar to pure Pb) and qualitatively different from the higher-binding-energy states seen in photoemission. This implies that there is a significant weight of the wave function responsible for the surface-state emission lying at the Pb atom sites, which are explicitly a two-dimensional array.

Additional evidence for the assignment of the 0.45 and 1.2-eV states to surface states comes from a detailed comparison between the angular distributions of photoemission from Ge(111)-$c(2\times8)$ and Pb/Ge(111)-$\sqrt{3}\times\sqrt{3}R30°$. This comparison is made in Fig. 6, which shows a selection of EDC's at two photon energies and various polar angles of emission. What is apparent in this figure is that there is almost a one-to-one correlation between spectral features in the clean Ge EDC's at each angle and the equivalent spectrum from the overlayer complex. This correlation can also be seen by comparing our polar distribution with unpolarized light (Fig. 3) with the data for Ge(111) of Bringans and Höchst.[25]

For clean Ge(111), two low-lying surface states have been identified by a number of experimental studies.[25,27,28] These states have been measured at 1.4 and 0.8 eV from the VBM. The polar-angle dependence of the intensity of the clean surface states is similar to that found in Pb/Ge (see Fig. 6 and Ref. 25). Our data for lead on germanium suggests that the state we see at 1.2 eV is related to the surface state at 1.4 eV in clean Ge. This conclusion is supported by a number of metal-semiconductor studies which show similar behavior.[14–16] Most of this work has been done on Si(111) surfaces, but there is a strong similarity to the present work on Ge(111). Overlayers of Al (Ref. 14), Ga (Ref. 15), and In (Ref. 16) on Si(111) have been studied using ARPES. All of these systems exhibit two surface state bands near the $\bar{\Gamma}'$ point of the $\sqrt{3}\times\sqrt{3}$ SBZ. The dispersion of surface states in Si(111)($\sqrt{3}\times\sqrt{3}$)-In, for example,[16] is similar to the 1.2-eV state dispersion in Pb/Ge(111) in the range of $\bar{M}'$-$\bar{\Gamma}'$-$\bar{M}'$ (Figs. 7 and 8). The bandwidth in the current case is smaller, however. It is important to note that while hydrogen chemisorption removes the low-lying surface states of clean Ge(111)-$c(2\times8)$,[25] chemisorption of lead simply shifts them in energy. The bonding of lead to the germanium surface involves covalent bonds that are similar to the bonding of surface atoms in the pure semiconductor. This implies that the surface states in clean and Pb-covered Ge have a common origin in an adatom overlayer structure.

The higher-binding-energy states shown in Fig. 7 appear to be related to bulk Ge band structure. With the exception of shifts to smaller binding energy of a few tenths of an eV, the dispersion of bands between 2 and 8 eV in Pb/Ge look remarkably similar to the clean surface. Our results include polarized spectra, which show additional features in the (2–3)-eV range when compared to the unpolarized data. We can make a detailed comparison between the bulklike bands in Pb/Ge(111) and those of the Ge(111) surface using the results of Bringans *et al.*[27] Near the $\bar{K}$ point there is a band in clean Ge(111) that occurs at -4.75 eV (Fig. 5 of Ref. 27). In the Pb/Ge(111) system, this band is shifted toward lower binding energy by 0.25 eV. Shifts of similar magnitude are seen in bulklike bands at other symmetry points. We note that the shape of the dispersion of the band near -4.75 eV is not altered significantly by addition of a (1×1) As overlayer[27] or by a $(\sqrt{3}\times\sqrt{3})$ Pb overlayer, which suggests that there is negligible contribution from surface orbitals to this band. The magnitude of the shifts

in energy of the bulklike bands in Pb/Ge(111) (0.25–0.3 eV) cannot be accounted for entirely by band bending, since the clean Ge(111)-$c(2\times8)$ VBM lies only 0.1 eV below the Fermi level.[21,25]

A portion of the measured band structure is reproduced along with the projected bulk Ge band structure in Fig. 8. The bulk band projection is bounded by the high-symmetry lines $\Gamma\rightarrow K\rightarrow X\rightarrow L\rightarrow W\rightarrow L\rightarrow\Gamma$ as shown in Fig. 4. The upper boundary of the projected bands shown in Fig. 8 are taken from the $\Gamma\rightarrow K\rightarrow X$ dispersions of Chekikowsky and Cohen, adjusted for the measured X_5 point from Chiang *et al.*[36] The symmetric upper band around the X point is due to the $W\rightarrow L$ dispersion which was taken from Grobman *et al.*[21] The band extending below 6 eV is the $\Gamma'_{25}\rightarrow X_1$ band, also from Chelikowsky and Cohen.[37] The holes in the upper valence band are located by reference to Bringans *et al.*[27] and Ivanov *et al.*[38] The measured bands from Pb/Ge(111) in the region below 2-eV BE follow the shape of the bulk dispersion projected into the $[1\bar{1}0]$ plane quite closely. There is no exact correspondence between the measured dispersion and any specific band along a high-symmetry direction, however, since both the perpendicular and parallel component of momentum is varied when the data is collected as a function of polar angle.

As mentioned above, the Pb overlayer can be disordered by raising the temperature of the substrate above $\approx 190\,^{\circ}$C. Bands with predominantly Pb character, such as the 0.45- and 1.2-eV states, are greatly reduced in intensity with increasing temperature,[35] whereas emission from bulklike bands are not as strongly affected. The origin of this difference lies in the widely differing Debye temperatures of substrate and overlayer, and provides a convenient way for establishing overlayer contribution to the measured band structure, without having to resort to different curves. Temperature-dependent spectra reported earlier[35] indicate that there is some overlayer contribution to the bands at 3.4- and 4.5-eV BE near $\mathbf{k}_{\parallel}=1.1$ Å^{-1} (see Figs. 7 and 8). Both of these bands have counterparts in the clean, bulk Ge(111) photoemission, but appear to partially mix with Pb states in this region of the Brillouin zone.

Emission from a broad state approximately 1 eV wide located at 7.5-eV Be was found in several of the spectra of Pb/Ge(111). A similar state has been identified by other groups in photoemission from clean Ge.[21,26] As seen in Fig. 10, the intensity of emission from this state is a strong function of the incident photon energy. A similar dependence, though somewhat less dramatic, has been seen in normal emission from clean Ge(111). In the clean system, this feature, and its intensity variation, were ascribed to a density-of-states effect[26] from bands near the bulk L point.[21] Such intensity variations are often associated with transitions for which the total momentum vector lies somewhere near a bulk high-symmetry point. In order to investigate the behavior of this state in more detail, the intensity was monitored as a function of initial momentum. First, a peak intensity was found by varying polar angle of collection for a fixed photon energy. The trajectory in $\mathbf{k}$ space is shown as a dashed line in Fig. 4, with a circle marking the $\mathbf{k}$ value resulting in maximum intensity. Next, both photon energy and polar angle were varied, so as to maintain constant $\mathbf{k}_{\parallel}$, resulting in the vertical trajectory shown. The actual EDC's generated are plotted in Fig. 10, and the integrated intensity of the 7.5-eV feature is shown as a function of photon energy in Fig. 11. The maximum emission intensity occurs at the $\mathbf{k}$ point marked as a square in Fig. 4. The values for $\mathbf{k}$ perpendicular were calculated assuming a free-electron final state, for which $|\mathbf{k}|=0.512(\hbar\omega-E_{\mathrm{BE}}+V_0)^{1/2}$. The trajectories shown in Fig. 4 used an inner potential of $V_0=7.7$ eV, a value that has been applied to previous clean Ge band-structure analyses.[26] A more recent study has found better agreement with experiment using a V_0 of 9.7 eV.[27] Using this value would shift the $\mathbf{k}$-perpendicular values plotted in Fig. 4 to slightly higher values. Also shown in Fig. 4 is the point at which maximum intensity from this band occurs in normal emission, taken from Chiang *et al.*[26] (triangle in Fig. 4). Despite the clear dependence on $k_{\perp}$ shown in Figs. 10 and 11, the maximum intensity does not occur near a bulk critical point, either for normal or off-normal emission. This suggests that the intensity dependence of this band is in fact dominated by relatively flat regions of the initial-state band structure, rather than originating in a final-state effect.

V. SUMMARY AND CONCLUSIONS

Monolayers of lead on Ge(111) can be grown with accurately reproducible coverages by monitoring the Auger electron yield. The Pb monolayer exhibits two surface-state bands lying in an absolute band gap of the projected bulk bands. The surface-state origin of these features in

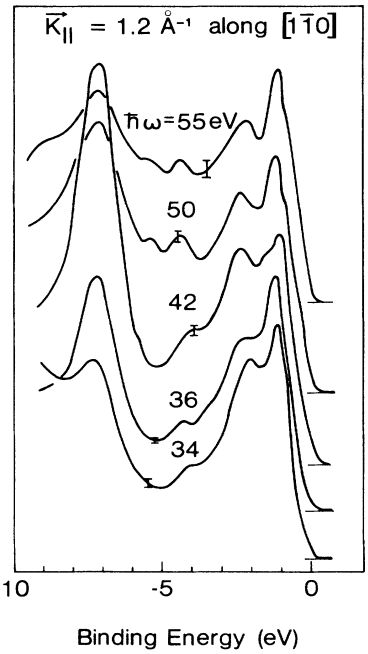

FIG. 10. Photon-energy-dependence emission from a broad state at 7.5-eV binding energy, for a fixed $\mathbf{k}_{\parallel}$. The polar angle of collection was varied with the photon energy to maintain constant parallel momentum.

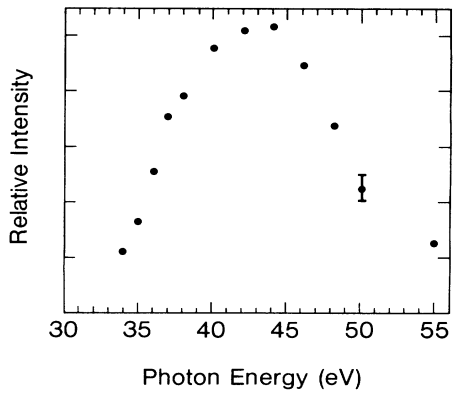

FIG. 11. Integrated intensity from the state at 7.5-eV binding energy and $|\mathbf{k}_{\parallel}| = 1.2$ Å^{-1} along $[1\bar{1}0]$ as a function of photon energy.

the spectra has been demonstrated by independently varying the perpendicular and parallel components of the electron momentum through the application of variable incident photon energy. These two states are split by 0.8 eV, with the higher-Be state showing a small bandwidth of 0.3 eV. The detailed dependence of photoemission from states in Pb/Ge(111) shows a striking correspondence to the reconstructed Ge(111)-$c(2\times8)$ surface. Both systems show two surface states located in the same region of $\mathbf{k}$ space. The polarization dependence of the surface states in Pb/Ge(111) and reconstructed germanium is also similar.

The Pb/Ge system forms a $\sqrt{3}\times\sqrt{3}$ overlayer, in common with several metal overlayers formed on Ge(111) and Si(111). A calculation by Northrup[39] accounts in part for the measured surface-state dispersion seen in $(\sqrt{3}\times\sqrt{3})$-metal/Si(111) overlayers, being particularly successful with Al/Si(111). The coverage in these overlayers is $\frac{1}{3}$, corresponding to a structure with only the open-circle overlayer atoms occupied in Fig. 1. The lowest-energy site in Northrup's calculation corresponds to the threefold occupied T_4 sites. The corner Pb atoms in Fig. 1 are shown on T_4 sites. However, the dispersion of surface states generated by $\sqrt{3}\times\sqrt{3}$ overlayer on threefold empty (H_3) sites is nearly identical to that for the T_4 sites, so that experimental energy dispersions alone cannot select between the two.[16]

While the absolute coverage in monolayer Pb is not known at this time, it is bounded by a minimum of $\frac{2}{3}$, and a maximum of $\frac{4}{3}$ by our measurements and from geometrical arguments based upon packing density. The present photoemission experiments argue for occupancy of the T_4 or H_3 threefold hollow sites, which accounts for the surface-state emission of the Pb-induced band at 1.2 eV. This band has significant p_z character, but does not vanish in forbidden geometry, so that there must also be p_x-p_y-like contributions to the wave function This interpretation is identical to that reached by Bringans *et al.* for an analogous surface state at 1.4 eV on clean Ge(111).[25] Northrup's calculations would suggest that this state is due to the overlap of substrate p_z orbitals with the Pb p_x-p_y orbitals in the T_4 site,[39] which is consistent with our experimental results for polarization and angle dependence. The similarity of the surface-state emission in Ge(111)-$c(2\times8)$ and Pb/Ge(111) then implies that in reconstructed clean Ge(111) there are Ge adatoms occupying the same threefold sites.

Our model for the structure of the saturated lead monolayer is as follows. The surface-state emission is explained by lead atoms occupying threefold sites in a $\sqrt{3}\times\sqrt{3}$ lattice. This accounts for a coverage of $\frac{1}{3}$, and saturates the dangling bonds of an ideal Ge(111) surface. If the lead adatom bonding at these sites results in motion of the nearest-neighbor Ge surface atoms, the remaining threefold sites will become inequivalent. Addition of further lead atoms in the coverage range from $\frac{2}{3}-1$ will occupy these sites with a different surface-substrate height, thereby preserving the $\sqrt{3}\times\sqrt{3}$ unit cell. The presence of two inequivalent threefold Pb-atom sites can account for the presence of the additional surface-state feature at 0.45 eV. For example, a similar shallow surface state in clean Ge at 0.8 eV has been associated with Ge rest-atom p_z dangling bonds.[27] This suggests that the state we find at 0.45 eV may be due to p_z orbitals of Pb atoms with a different height above the surface from the corner atoms in the unit cell.

ACKNOWLEDGMENTS

We are grateful for the assistance of the staff of the University of Wisconsin Synchrotron Radiation Center (Stoughton, WI). This work was supported by the National Science Foundation (Division of Materials Science) under Grant No. DMR-84-15158, by the University of Wisconsin–Milwaukee Graduate Research Program, and by the University of Texas Joint Services Electronics Program under Grant No. F49620-86-0045. The Synchrotron Radiation Center is supported under Grant. No. DMR-80-20164. Valuable assistance was provided by Y. C. Chou and M. Thompson.

*Author to whom correspondence should be addressed.

[1] V. Yu. Aristov, N. I. Golovko, V. A. Grazhulis, Yu. A. Ossipyan, and V. I. Talyanskii, Surf. Sci. **117**, 204 (1982).
[2] R. J. Phaneuf and M. B. Webb, Surf. Sci. **164**, 167 (1985).
[3] J. M. Nicholls, G. V. Hansson, R. I. G. Uhrberg, and S. A. Flodström, Phys. Rev. B **27**, 2594 (1983).
[4] M. Taubenblatt, E. So, P. Sih, A. Kahn, and P. Mark, J. Vac. Sci. Technol. **15**, 1143 (1978).
[5] D. J. Chadi and C. Chiang, Phys. Rev. B **23**, 1843 (1981).
[6] W. S. Yang and F. Jona, Phys. Rev. B **29**, 899 (1984).
[7] K. Takayanagi and Y. Tanishiro, Phys. Rev. B **34**, 1034 (1986).
[8] K. Takayanagi, Y. Tanishiro, M. Takahashi, and S. Takahashi, J. Vac. Sci. Technol. A **3**, 1502 (1985).
[9] R. S. Becker, J. A. Golovchenko, E. G. McRae, and B. S.

Swartzentruber, Phys. Rev. Lett. **55**, 2028 (1985).
[10]Sn/Ge(111) structural work can be found in T. Ichikawa and S. Ino, Surf. Sci. **105**, 395 (1981); K. Nakamura, K. Ohtumi, and S. Sugano, J. Phys. C **17**, 5645 (1984); K. Higashiyama, S. Kono, H. Sakurai, and T. Sagawa, Solid State Commun. **49**, 253 (1984).
[11]J. J. Metois and G. LeLay, Surf. Sci. **133**, 422 (1983).
[12]T. Ichikawa, Solid State Commun. **46**, 827 (1983); **49**, 59 (1984).
[13]G. LeLay and J. M. Metois, J. Phys. (Paris) Colloq. **45**, C5-427 (1984); G. LeLay and Z. Imam, Surf. Sci. **154**, 90 (1985).
[14]R. I. G. Uhrberg, G. V. Hansson, J. M. Nicholls, P. E. Persson, and S. A. Flodström, Phys. Rev. B **31**, 3805 (1985).
[15]K. Higashiyama, S. Kono, and T. Sagawa, Surf. Sci. **175**, L794 (1986); T. Kinoshita, S. Kono, and T. Sagawa, Phys. Rev. B **34**, 3011 (1986).
[16]J. M. Nicholls, P. Martensson, G. V. Hansson, and J. E. Northrup, Phys. Rev. B **32**, 1333 (1985).
[17]E. Suliga and M. Henzler, J. Phys. C **16**, 1543 (1983).
[18]M. Hansen, *Constitution of Binary Alloys* (McGraw-Hill, New York, 1958), p. 771.
[19]Related x-ray work has been done on Pb-Ge superlattices: R. H. Willens, A. Kornblit, L. R. Testardi, and S. Nakahara, Phys. Rev. B **25**, 290 (1982).
[20]H. Li and B. P. Tonner (unpublished).
[21]W. D. Grobman, D. E. Eastman, and J. L. Freeouf, Phys. Rev. B **12**, 4405 (1975).
[22]J. E. Rowe, Solid State Commun. **17**, 673 (1975).
[23]T. Murotani, K. Fujiwara, and M. Nishijima, Phys. Rev. B **12**, 2424 (1975).
[24]F. J. Himpsel, D. E. Eastman, P. Hermann, B. Reihl, C. W. White, and D. M. Zehner, Phys. Rev. B **24**, 1120 (1981).
[25]R. D. Bringans and H. Höchst, Phys. Rev. B **25**, 1081 (1982).
[26]A. L. Wachs, T. Miller, T. C. Hsieh, A. P. Shapiro, and T.-C. Chiang, Phys. Rev. B **32**, 2326 (1985).
[27]R. D. Bringans, R. I. G. Uhrberg, and R. Z. Bachrach, Phys. Rev. B **34**, 2373 (1986).
[28]J. M. Nicholls, G. V. Hansson, R. I. G. Uhrberg, and S. A. Flodström, Phys. Rev. B **33**, 5555 (1986).
[29]G. K. Ovrebo and J. L. Erskine, J. Electron. Spectrosc. Related Phenom. **24**, 189 (1981).
[30]B. P. Tonner, Nucl. Instrum. Methods **172**, 133 (1980).
[31]See, for example, E. Bauer, H. Poppa, G. Todd, and F. Bonczek, and J. Appl. Phys. **45**, 5164 (1974).
[32]A similar LEED pattern was found in the epitaxial growth of Pb on Ag(111): C. H. Chen and F. J. Sansalone, Surf. Sci. **163**, L688 (1985).
[33]K. Horn, B. Reihl. A. Zartner, D. E. Eastman, K. Herman, and J. Noffke, Phys. Rev. B **30**, 1711 (1984).
[34]A. Liebsch, Phys. Rev. B **32**, 1203 (1974).
[35]B. P. Tonner, H. Li, M. Robrecht, Y. C. Chou, M. Onellion, and J. Erskine, Phys. Rev. B **34**, 4386 (1986).
[36]T. C. Hsieh, T. Miller, and T.-C. Chiang, Phys. Rev. B **30**, 7005 (1984).
[37]J. R. Chelikowsky and M. L. Cohen, Phys. Rev. B **14**, 556 (1976).
[38]I. Ivanov, A. Mazur, and J. Pollman, Surf. Sci. **92**, 365 (1980).
[39]J. E. Northrup, Phys. Rev. Lett. **57**, 154 (1986).